SIAM J. APPL. MATH.
Vol. 65, No. 1, pp. 131–151
© 2004 Society for Industrial and Applied Mathematics

FRONT BIFURCATIONS IN AN EXCITATORY NEURAL NETWORK*

PAUL C. BRESSLOFF† AND STEFANOS E. FOLIAS†

Abstract. We show how a one-dimensional excitatory neural network can exhibit a symmetry breaking front bifurcation analogous to that found in reaction diffusion systems. This occurs in a homogeneous network when a stationary front undergoes a pitchfork bifurcation leading to bidirectional wave propagation. We analyze the dynamics in a neighborhood of the front bifurcation using perturbation methods, and we establish that a weak input inhomogeneity can induce a Hopf instability of the stationary front, leading to the formation of an oscillatory front or breather. We then carry out a stability analysis of stationary fronts in an exactly solvable model and use this to derive conditions for oscillatory fronts beyond the weak input regime. In particular, we show how wave propagation failure occurs in the presence of a large stationary input due to the pinning of a stationary front; a subsequent reduction in the strength of the input then generates a breather via a Hopf instability of the front. Finally, we derive conditions for the locking of a traveling front to a moving input, and we show how locking depends on both the amplitude and velocity of the input.

Key words. traveling waves, neural networks, cortical models, front bifurcations, inhomogeneous media

AMS subject classification. 92C20

DOI. 10.1137/S0036139903434481

1. Introduction.

Nonlinear integro-differential equations of the form

$$\tau_s \frac{\partial u(x,t)}{\partial t} = -u(x,t) + \int_{-\infty}^{\infty} w(x-x') f(u(x',t)) dx' - \beta v(x,t) + I(x),$$

$$\frac{1}{\varepsilon}\frac{\partial v(x,t)}{\partial t} = -v(x,t) + u(x,t) \tag{1.1}$$

have arisen as continuum models of one-dimensional cortical tissue [1, 12], in which $u(x,t)$ is a neural field that represents the local activity of a population of excitatory neurons at position $x \in \mathbf{R}$, $I(x)$ is an external input current, τ_s is a synaptic time constant (assuming first-order synapses), $f(u)$ denotes the output firing rate function, and $w(x-x')$ is the strength of connections from neurons at x' to neurons at x. The distribution $w(x)$ is taken to be a positive, even function of x. The neural field $v(x,t)$ represents some form of negative feedback mechanism such as spike frequency adaptation or synaptic depression, with β, ε determining the relative strength and rate of feedback. If additional nonlocal terms in v are introduced, then v represents instead the activity of a population of inhibitory neurons [17, 1]. The nonlinear function f is usually taken to be a smooth sigmoid function

$$f(u) = \frac{1}{1+\mathrm{e}^{-\gamma(u-\kappa)}} \tag{1.2}$$

with gain γ and threshold κ. The units of time are fixed by setting $\tau_s = 1$; a typical value of τ_s is 10 msec. It can be shown [12] that there is a direct link between the above model and experimental studies of wave propagation in cortical slices where synaptic inhibition is pharmacologically blocked [4, 7, 18]. Since there is strong vertical

*Received by the editors September 8, 2003; accepted for publication (in revised form) May 12, 2004; published electronically September 24, 2004. This research was supported by NSF grant DMS-0209824.

http://www.siam.org/journals/siap/65-1/43448.html

†Department of Mathematics, University of Utah, 155 South 1400 East 233 JWB, Salt Lake City, UT 84112 (bressloff@math.utah.edu, sfolias@math.utah.edu).

coupling between cortical layers, it is possible to treat a thin cortical slice as an effective one-dimensional medium. Analysis of the model provides valuable information regarding how the speed of a traveling wave, which is relatively straightforward to measure experimentally, depends on various features of the underlying cortical circuitry.

A number of previous studies have considered the existence and stability of traveling wave solutions of (1.1) in the case of a uniform input I, which is equivalent to a shift in the threshold κ. In particular, it has been shown that in the absence of any feedback ($\beta = 0$), the resulting scalar network can support the propagation of traveling fronts [5, 10], whereas traveling pulses tend to occur when there is significant negative feedback [17, 1, 12]. In this paper, we show that such feedback can also have a nontrivial effect on the propagation of traveling fronts. This is due to the occurrence of a symmetry breaking front bifurcation analogous to that found in reaction diffusion systems [14, 8, 16, 9, 2, 15, 13, 11]. We begin by deriving conditions for the existence of traveling wavefronts in the case of a homogeneous network (section 2). We then carry out a perturbation expansion in powers of the wavespeed c to show that a stationary front can undergo a supercritical pitchfork bifurcation at a critical rate of negative feedback, leading to bidirectional front propagation (section 3). As in the case of reaction diffusion systems, the front bifurcation acts as an organizing center for a variety of nontrivial dynamics including the formation of oscillatory fronts or breathers. We show how the latter can occur through a Hopf bifurcation from a stationary front in the presence of a weak stationary input inhomogeneity (section 4). Finally, we analyze the existence and stability of stationary fronts in an exactly solvable model, which is obtained by taking the high gain limit $\gamma \to \infty$ of the sigmoid function f such that $f(u) = H(u - \kappa)$, where H is the Heaviside function (section 5). As briefly reported elsewhere [3], the exactly solvable model allows us to study oscillatory fronts beyond the weak input regime. Rather than perturbing about the homogeneous case, we now consider a large input amplitude for which wave propagation failure occurs due to the pinning of a stationary front. A subsequent reduction in the amplitude of the input then induces a Hopf instability, leading to the formation of a breather. We conclude our analysis of the exactly solvable model by deriving conditions for the locking of a traveling front to a moving input, and we show how locking depends on both the amplitude and speed of the input.

The major advantage of the exactly solvable model is that it allows us to explicitly determine the existence and stability of stationary and traveling fronts in the presence of external inputs, without any restrictions on the size of the input. However, it has the disadvantage of restricting the nonlinear function f to be a step function. This is less realistic than the smooth nonlinearity (1.2), which matches quite well the input–output characteristics of populations of neurons. The lack of smoothness also makes it difficult to carry out a nonlinear analysis in order to determine whether or not the Hopf instability is supercritical, for example. As we show in this paper, such an analysis can be carried out for smooth f provided that the input amplitude is sufficiently weak. The fact that the nonlocal integro-differential equation (1.1) exhibits behavior similar to a reaction–diffusion system might not be surprising, particularly given that for the exponential weight distribution $w(x) = \mathrm{e}^{-|x|}$, equation (1.1) can be reduced to a PDE of the reaction–diffusion type. It is important to emphasize, however, that our results hold for a more general class of weight distribution $w(x)$ for which a corresponding (finite-order) PDE cannot be constructed. Hence, the analysis is a nontrivial extension of known results for reaction–diffusion equations.

2. Traveling fronts in a homogeneous network. In this section we investigate the existence of traveling front solutions of (1.1) for homogeneous inputs by combining results on scalar networks [5] with an extension of the analysis of front bifurcations in nonscalar reaction–diffusion equations [8, 2].

2.1. The scalar case. The existence of traveling front solutions in scalar, homogeneous networks was previously analyzed by Ermentrout and McLeod [5]. Their analysis can be applied to a scalar version of (1.1) obtained by taking $\varepsilon \to \infty$ so that $v = u$ and setting $I(x) = -h$ with h a constant input. This leads to the scalar integro-differential equation

$$\frac{\partial u(x,t)}{\partial t} = -(1+\beta)u(x,t) + \int_{-\infty}^{\infty} w(x-x')f(u(x',t))dx' - h. \tag{2.1}$$

Without loss of generality we choose h such that $\kappa = 0$ in the sigmoid function (1.2). The weight distribution w is assumed to be a positive, even, continuously differentiable function of x with unit normalization $\int_{-\infty}^{\infty} w(y)dy = 1$. Suppose that the function

$$F_{h,\beta}(u) = f(u) - (1+\beta)u - h \tag{2.2}$$

has precisely three zeros at $u = U_{\pm}(h,\beta), U_0(h,\beta)$ with $U_- < U_0 < U_+$ and $F'_{h,\beta}(U_{\pm}) < 0$. It can then be shown that (modulo uniform translations) there exists a unique traveling front solution of (2.1) such that $u(x,t) = U(\xi)$, $\xi = x - ct$, with $U(\xi) \to U_{\pm}$ as $\xi \to \mp\infty$ [5]. Moreover, the speed of the wave satisfies

$$c = c(h,\beta) = \frac{\Gamma_{h,\beta}}{\int_{-\infty}^{\infty} u'^2 f'(u)d\xi}, \tag{2.3}$$

where

$$\Gamma_{h,\beta} = \int_{U_-}^{U_+} F_{h,\beta}(u)du. \tag{2.4}$$

Since the denominator of (2.3) is positive definite, the sign of c is determined by the sign of the coefficient $\Gamma_{h,\beta}$. In particular, suppose that $h = 0.5$ and f is given by the sigmoid function (1.2) so that $f(u) - h = \tanh(u/2\gamma)/2$. It follows that, for $0 < 1+\beta < \gamma/4$, there exists a pair of stable homogeneous fixed points with $U_- = -U_+$, which in turn implies that $\Gamma_{h,\beta} = 0$ and the front solution is stationary; see Figure 2.1. The corresponding function $F_{h,\beta}(u)$ has the inflection symmetry $F_{h,\beta}(-u) = -F_{h,\beta}(u)$. Note that the stationary solution of (2.1) is also an ε-independent solution of the full system (1.1) with $I(x) = -h$, but it is not necessarily the only solution (see below).

2.2. The regime $\varepsilon \gg 1$. In the large ε regime, the neural field v varies on a much faster time scale than u. Introducing the stretched time coordinate $\tau = t/\delta$ with $\delta = \varepsilon^{-1} \ll 1$, we have

$$\frac{\partial u(x,\tau)}{\partial \tau} = \delta\left(-u(x,\tau) + \int_{-\infty}^{\infty} w(x-x')f(u(x',\tau))dx' - \beta v(x,\tau) - h\right),$$

$$\frac{\partial v(x,\tau)}{\partial \tau} = -v(x,\tau) + u(x,\tau). \tag{2.5}$$

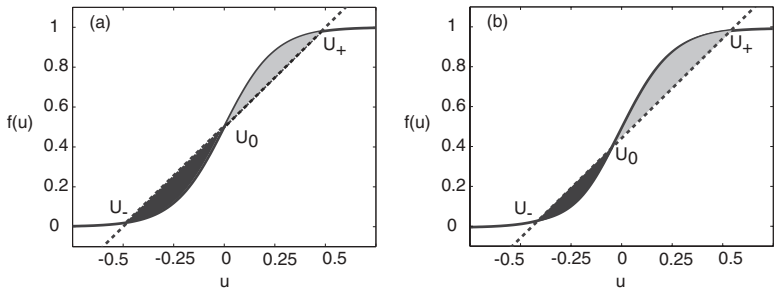

FIG. 2.1. *Balance condition for the speed of a traveling wavefront in a scalar excitatory network with* $u(x,t) = U(x-ct)$ *such that* $U(\mp\infty) = U_\pm$. *The solid curve is* $f(u) = 1/(1+\mathrm{e}^{-\gamma u})$ *with* $\gamma = 8$, *and the dashed line is* $g(u) = (1+\beta)u + h$. *The wavespeed* c *is positive (negative) if the gray shaded area is larger (smaller) than the black shaded area.* (a) $h = 0.5$, $\beta = 0.5$ *such that* $c = 0$. (b) $h = 0.4$, $\beta = 0.5$ *such that* $c > 0$.

To leading order in δ, u is independent of τ so that we can explicitly solve for v according to

$$v(x,t) = v_0(x)\mathrm{e}^{-\varepsilon t} + u(x,t)(1-\mathrm{e}^{-\varepsilon t}). \tag{2.6}$$

Thus after an initial transient of duration $t \sim \mathcal{O}(\varepsilon^{-1})$, the field v adiabatically follows the field u, with the latter evolving according to the scalar equation (2.1). It follows that in the large ε regime there exists a unique traveling wave solution of the full system with $(u(x,t), v(x,t)) = (U(x-ct), V(x-ct))$ such that $(U,V) \to (U_\pm, U_\pm)$ as $\xi \to \mp\infty$ and $c = c(h,\beta)$, $U_\pm = U_\pm(h,\beta)$. The front is stable in the large ε regime provided that the solution of the corresponding scalar equation is stable, which is found to be the case numerically. If $\Gamma_{h,\beta} = 0$, then the front is stationary and persists for all ε but may become unstable as ε is reduced.

2.3. The regime $0 < \varepsilon \ll 1$. In the small ε regime, additional front solutions can be constructed that connect the two fixed points $(u,v) = (U_\pm(h,\beta), U_\pm(h,\beta))$. This follows from the observation that the neural field v remains approximately constant on the length scale over which u varies, that is, within the transition layer of the front. Suppose that the system is prepared in the down state (U_-, U_-) and is perturbed on its left-hand side to induce a transition to the upper state (U_+, U_+). In this case $v \approx U_-$ within the transition layer, and this generates a front propagating to the right whose speed is approximately given by (2.3) with $h \to h + \beta U_-$, that is, $c = c(h + \beta U_-, 0)$. If, on the other hand, the system is prepared in the up state (U_+, U_+) and is perturbed on its right-hand side to induce a transition to the down state (U_-, U_-), then a left-propagating front is generated with $c = c(h + \beta U_+, 0)$. Note from (2.4) that

$$\Gamma_{h+\beta U_-,0} > \Gamma_{h,\beta} + \beta \int_{U_-}^{U_+} (u - U_-)du, \quad \Gamma_{h+\beta U_+,0} < \Gamma_{h,\beta} + \beta \int_{U_-}^{U_+} (u - U_+)du \tag{2.7}$$

so that $\Gamma_{h+\beta U_-,0} > \Gamma_{h,\beta} > \Gamma_{h+\beta U_+,0}$. Hence, the existence of fronts propagating in opposite directions clearly holds when h, β are chosen such that $\Gamma_{h,\beta} = 0$.

3. Front bifurcation. The above analysis suggests that if $\Gamma_{h,\beta} = 0$, then at some critical rate of feedback $\varepsilon = \varepsilon_c$, a pair of counterpropagating fronts bifurcate

from a stationary front. Moreover, all the front solutions have the same asymptotic behavior $(U(\xi), V(\xi)) \to (U_\pm, U_\pm)$ as $\xi \to \mp\infty$. Following along lines analogous to Hagberg and Meron [8], we carry out a perturbation expansion in powers of the speed c about this critical point, and we show that the stationary solution undergoes a pitchfork bifurcation.

First, set $I(x) = -h$ and $(u(x,t), v(x,t)) = (U(x-ct), V(x-ct))$ in (1.1) to obtain the pair of equations

$$\begin{aligned} -cU' &= -U + w * f(U) - \beta V, \\ -cV' &= \varepsilon[-V + U], \end{aligned} \tag{3.1}$$

where $U' = dU/d\xi$ and $*$ denotes the convolution operator,

$$w * U = \int_{-\infty}^{\infty} w(\xi - \xi')U(\xi')d\xi'. \tag{3.2}$$

Suppose that β and h are fixed such that $\Gamma_{h,\beta} = 0$, and denote the corresponding stationary solution by $(\overline{U}, \overline{V})$. Expand the fields U, V as power series in c:

$$\begin{aligned} U(\xi) &= \overline{U}(\xi) + cU_1(\xi) + c^2U_2(\xi) + \cdots, \\ V(\xi) &= \overline{V}(\xi) + cV_1(\xi) + c^2V_2(\xi) + \cdots. \end{aligned} \tag{3.3}$$

Note that the higher order terms $U_n(\xi), V_n(\xi)$, $n \geq 1$, should all decay to zero as $\xi \to \pm\infty$, since the stationary solution already has the correct asymptotic behavior. Also expand ε according to

$$\varepsilon = \varepsilon_c + c\varepsilon_1 + c^2\varepsilon_2 + \cdots. \tag{3.4}$$

Substitute these expansions into (3.1) and Taylor expand the nonlinear function $f(U)$ about $\overline{U}$:

$$f(U) = f(\overline{U}) + \sum_{n\geq 1} \overline{f}_n(U - \overline{U})^n, \quad \overline{f}_n = \frac{1}{n!}\frac{d^n f}{dU^n}\bigg|_{U=\overline{U}}. \tag{3.5}$$

Collecting all terms at successive orders of c then generates a hierarchy of equations for the perturbative corrections U_n, V_n. The lowest order equation recovers the conditions for a stationary solution:

$$\begin{aligned} (1+\beta)\overline{U} + h &= w * f(\overline{U}), \\ \overline{V} &= \overline{U}. \end{aligned} \tag{3.6}$$

At order c we have

$$\begin{aligned} -\overline{U}' &= -U_1 + w * [\overline{f}_1 U_1] - \beta V_1, \\ -\overline{V}' &= \varepsilon_c[-V_1 + U_1] + \varepsilon_c[-\overline{V} + \overline{U}]. \end{aligned} \tag{3.7}$$

The term $-\beta V_1$ in the first line can be eliminated using the second. Since $\overline{V} = \overline{U}$, we thus find that

$$\mathcal{M}U_1 = \left(\frac{\beta}{\varepsilon_c} - 1\right)\overline{U}', \quad V_1 = U_1 + \frac{\overline{U}'}{\varepsilon_c}, \tag{3.8}$$

where $\mathcal{M}$ is the linear operator

$$\mathcal{M}U = -(1+\beta)U + w * [\overline{f}_1 U]. \tag{3.9}$$

Since the functions $U_n(\xi), V_n(\xi)$ decay to zero as $\xi \to \pm\infty$, we will assume that $\mathcal{M}$ acts on the space $L^2(\mathbf{R})$ and introduce the generalized inner product

$$\langle U|V\rangle = \int_{-\infty}^{\infty} f'(\overline{U}(\xi))U(\xi)V(\xi)d\xi \tag{3.10}$$

for all $U, V \in L^2(\mathbf{R})$. With respect to this space, $\mathcal{M}$ is self-adjoint and has the null vector $\overline{U}'$[1]:

$$\mathcal{M}\overline{U}' = \mathcal{M}^\dagger \overline{U}' = 0. \tag{3.11}$$

Applying the Fredholm alternative to (3.8) then gives the solvability condition

$$\langle \overline{U}'|\overline{U}'\rangle \left(\frac{\beta}{\varepsilon_c} - 1\right) = 0. \tag{3.12}$$

Since $f'(\overline{U}(\xi)) > 0$ for all ξ, it follows that $\langle \overline{U}'|\overline{U}'\rangle > 0$ and thus $\varepsilon_c = \beta$. This in turn means that $\mathcal{M}U_1 = 0$ and hence $U_1 = A\overline{U}'$ for some constant A. Since $\overline{U}'$ is the generator of uniform translations, we are free to choose the origin such that $A = 0$. Under this choice,

$$U_1 = 0, \quad V_1 = \frac{\overline{U}'}{\varepsilon_c}. \tag{3.13}$$

At order c^2 we obtain

$$\begin{aligned} -U_1' &= \mathcal{M}U_2 + \beta[-V_2 + U_2] + w * [\overline{f}_2 U_1^2], \\ -V_1' &= \varepsilon_c[-V_2 + U_2] + \varepsilon_1[-V_1 + U_1] + \varepsilon_2[-\overline{V} + \overline{U}]. \end{aligned} \tag{3.14}$$

Substituting for $-V_2 + U_2$ in the first line, taking $\overline{V} = \overline{U}$, $\beta = \varepsilon_c$, and using equation (3.13) then gives

$$\mathcal{M}U_2 = \frac{1}{\varepsilon_c}\left(\overline{U}'' - \varepsilon_1 \overline{U}'\right), \quad V_2 = U_2 + \frac{1}{\varepsilon_c^2}(\overline{U}'' - \varepsilon_1 \overline{U}'). \tag{3.15}$$

Applying the Fredholm alternative to (3.15) yields the solvability condition

$$\langle \overline{U}'|\overline{U}''\rangle = \varepsilon_1 \langle \overline{U}'|\overline{U}'\rangle. \tag{3.16}$$

In order to evaluate the inner product $\langle \overline{U}'|\overline{U}''\rangle$, we use the result

$$(1+\beta)\frac{d^2\overline{U}}{d\xi^2} = \int_{-\infty}^{\infty} w(\xi - \xi')\frac{d^2 f(\overline{U}(\xi'))}{d{\xi'}^2}d\xi', \tag{3.17}$$

[1] We could equally well proceed by taking the standard inner product $\langle U|V\rangle = \int_{-\infty}^{\infty} U(\xi)V(\xi)d\xi$. The adjoint of $\mathcal{M}$ is then given by $\mathcal{M}^\dagger U = -(1+\beta)U + \overline{f}_1 w * U$, which has the null vector $\overline{f}_1\overline{U}'$ where $\overline{f}_1 = f'(\overline{U})$.

which follows from differentiating (3.6) with respect to ξ and using the asymptotic properties of w. Then

$$\begin{aligned}\langle \overline{U}' | \overline{U}'' \rangle &= \int_{-\infty}^{\infty} f'(\overline{U}(\xi))\overline{U}'(\xi)\overline{U}''(\xi)d\xi \\ &= \int_{-\infty}^{\infty} \frac{df(\overline{U}(\xi))}{d\xi}\overline{U}''(\xi)d\xi \\ &= \frac{1}{1+\beta}\int_{-\infty}^{\infty}\int_{-\infty}^{\infty} \frac{df(\overline{U}(\xi))}{d\xi} w(\xi-\xi')\frac{d^2 f(\overline{U}(\xi'))}{d\xi'^2}d\xi' d\xi \\ &= \frac{1}{1+\beta}\int_{-\infty}^{\infty}\int_{-\infty}^{\infty} \frac{df(\overline{U}(\xi))}{d\xi} w'(\xi-\xi')\frac{df(\overline{U}(\xi'))}{d\xi'}d\xi' d\xi \\ &= 0, \end{aligned} \tag{3.18}$$

since $w'(\xi)$ is an odd function of ξ. Hence, $\varepsilon_1 = 0$ and

$$\mathcal{M}U_2 = \frac{\overline{U}''}{\varepsilon_c}, \quad V_2 = U_2 + \frac{\overline{U}''}{\varepsilon_c^2}. \tag{3.19}$$

At order c^3 we obtain

$$\begin{aligned} -U_2' &= \mathcal{M}U_3 + \beta[-V_3 + U_3] + 2w * [\overline{f}_2 U_1 U_2] + w * [\overline{f}_3 U_1^3], \\ -V_2' &= \varepsilon_c[-V_3 + U_3] + \varepsilon_1[-V_2 + U_2] + \varepsilon_2[-V_1 + U_1] + \varepsilon_3[-\overline{V} + \overline{U}]. \end{aligned} \tag{3.20}$$

Substituting for $-V_2 + U_2$ in the first line, taking $\overline{V} = \overline{U}$, $\beta = \varepsilon_c$, $\varepsilon_1 = 0$, and using (3.13) and (3.19) then gives

$$\mathcal{M}U_3 = \frac{1}{\varepsilon_c^2}\left(\overline{U}''' - \varepsilon_2\varepsilon_c\overline{U}'\right), \quad V_3 = U_3 + \frac{1}{\varepsilon_c^3}(\overline{U}''' + \varepsilon_c^2 U_2' - \varepsilon_2\varepsilon_c\overline{U}'). \tag{3.21}$$

Applying the Fredholm alternative to (3.21) yields the solvability condition

$$\varepsilon_2 = \frac{\langle \overline{U}' | \overline{U}''' \rangle}{\varepsilon_c \langle \overline{U}' | \overline{U}' \rangle} < 0. \tag{3.22}$$

The sign of ε_2 can be determined using (3.17),

$$\begin{aligned}\langle \overline{U}' | \overline{U}''' \rangle &= \int_{-\infty}^{\infty} f'(\overline{U}(\xi))\overline{U}'(\xi)\overline{U}'''(\xi)d\xi \\ &= \int_{-\infty}^{\infty} \frac{df(\overline{U}(\xi))}{d\xi}\overline{U}'''(\xi)d\xi \\ &= -\int_{-\infty}^{\infty} \frac{d^2 f(\overline{U}(\xi))}{d\xi^2}\overline{U}''(\xi)d\xi \\ &= -\frac{1}{1+\beta}\int_{-\infty}^{\infty}\int_{-\infty}^{\infty} \frac{d^2 f(\overline{U}(\xi))}{d\xi^2} w(\xi-\xi')\frac{d^2 f(\overline{U}(\xi'))}{d\xi'^2}d\xi' d\xi \\ &< 0, \end{aligned} \tag{3.23}$$

since $w(\xi)$ is an even, monotonically decreasing function of $|\xi|$. Hence $\varepsilon_2 < 0$.

Combining these various results, we find that

$$\begin{aligned} U(\xi) &= \overline{U}(\xi) + \mathcal{O}(c^2), \\ V(\xi) &= \overline{U}(\xi) + \frac{c}{\varepsilon_c}\overline{U}'(\xi) + \mathcal{O}(c^2), \end{aligned} \tag{3.24}$$

and

$$\varepsilon = \varepsilon_c + c^2\varepsilon_2 + \mathcal{O}(c^3). \tag{3.25}$$

Equation (3.25) implies that the stationary front undergoes a pitchfork bifurcation, which is supercritical since $\varepsilon_2 < 0$. (This assumes of course that the stationary front is stable for $\varepsilon > \varepsilon_c$. This can be confirmed numerically, and also proven analytically in the high gain limit; see section 5.) Close to the bifurcation point the shape of the propagating fronts is approximately the same as the stationary front, except that the recovery variable V is shifted relative to U by an amount proportional to the speed c, that is,

$$U(\xi) \approx \overline{U}(\xi), \quad V(\xi) \approx \overline{U}(\xi + c/\varepsilon_c). \tag{3.26}$$

An analogous result was previously obtained for reaction–diffusion equations [8]. It is important to emphasize that the occurrence of a pitchfork bifurcation from a stationary front does not require any underlying inflection symmetries of the nonlinear function f (see also [2]). We only require that the scalar equation (2.1) supports a stationary front for appropriate choices of h, β. The fact that the weight distribution $w(x)$ is even means that there must be a pitchfork bifurcation from a stationary solution rather than a transcritical bifurcation as in the case of a nonsymmetric w.

4. The effect of a weak input inhomogeneity. Now suppose that both ε and h are allowed to vary. We then expect a codimension 2 cusp bifurcation in which the pitchfork bifurcation unfolds into a saddle-node bifurcation, with the stationary front replaced by a traveling front in the large ε regime. More interestingly, as in the case of reaction–diffusion systems [16, 9, 2], the pitchfork bifurcation acts as an organizing center for a variety of dynamical phenomena, including the formation of breathers due to the presence of a weak input inhomogeneity or due to curvature (in the case of two spatial dimensions). These breathers consist of periodic reversals in propagation that can be understood in terms of a dynamic transition between the pair of counterpropagating fronts that is induced by the weak intrinsic perturbation. Such a transition involves an interaction between a translational degree of freedom and an order parameter that determines the direction of propagation. In order to unravel this interaction, it is necessary to extend the perturbation analysis of section 3 along lines analogous to previous treatments of reaction–diffusion systems [16, 9, 2].

Suppose that the system (1.1) undergoes a pitchfork bifurcation from a stationary state when $\varepsilon = \varepsilon_c = \beta$ and $I(x) = -h$. Introduce the small parameter δ according to $\varepsilon - \varepsilon_c = \delta^2\chi$ and introduce a weak input inhomogeneity by taking $I(x) = -h + \delta^3\eta(x)$. Since any fronts are slowly propagating, we rescale time according to $\tau = \delta t$ so that (1.1) becomes

$$\begin{aligned} \delta\frac{\partial u(x,\tau)}{\partial \tau} &= -u(x,t) + \int_{-\infty}^{\infty} w(x-x')f(u(x',\tau))dx' - \beta v(x,\tau) - h + \delta^3\eta(x), \\ \delta\frac{\partial v(x,\tau)}{\partial \tau} &= (\varepsilon_c + \delta^2\chi)\left[-v(x,\tau) + u(x,\tau)\right]. \end{aligned} \tag{4.1}$$

Motivated by (3.24), we introduce the ansatz that, sufficiently close to the pitchfork bifurcation, the solutions of (4.1) can be expanded in the form

$$\begin{aligned} u(x,\tau) &= \overline{U}(x-p(\tau)) + \delta^2 u_2(x,\tau) + \delta^3 u_3(x,\tau) + \cdots, \\ v(x,\tau) &= \overline{U}(x-p(\tau)) + \delta\frac{a(\delta\tau)}{\varepsilon_c}\overline{U}'(x-p(\tau)) + \delta^2 v_2(x,\tau) + \delta^3 v_3(x,\tau) + \cdots. \end{aligned} \tag{4.2}$$

Here p is identified with the translational degree of freedom, whereas a represents the order parameter associated with changes in propagation direction. Note that a is assumed to evolve on a slower time scale than p. We now substitute the ansatz (4.2) into (4.1) and expand in powers of δ along lines similar to the perturbation calculation of section 3.

At order δ we find that

$$p_\tau = a, \tag{4.3}$$

where $p_\tau = dp/d\tau$. At order δ^2 we obtain the pair of equations

$$\mathcal{M}u_2 = a^2\frac{\overline{U}''}{\varepsilon_c}, \qquad v_2 = u_2 + a^2\frac{\overline{U}''}{\varepsilon_c^2} \tag{4.4}$$

after setting $p_\tau = a$. The solvability condition for (4.4) is automatically satisfied. At order δ^3 we have

$$\begin{aligned} \frac{\partial u_2}{\partial\tau} &= \mathcal{M}u_3 + \beta[-v_3 + u_3] + \eta, \\ \frac{\partial v_2}{\partial\tau} + \frac{\overline{U}'a_{\hat\tau}}{\varepsilon_c} &= \varepsilon_c[-v_3 + u_3] - a\chi\frac{\overline{U}'}{\varepsilon_c} \end{aligned} \tag{4.5}$$

with $\hat\tau = \delta\tau$. Using (4.4), the following equation for u_3 is obtained:

$$\mathcal{M}u_3 = \frac{1}{\varepsilon_c^2}\left(a^3\overline{U}''' - a\chi\varepsilon_c\overline{U}' - a_{\hat\tau}\varepsilon_c\overline{U}'\right) - \eta. \tag{4.6}$$

Applying the Fredholm alternative to (4.6) yields an amplitude equation for a:

$$a_{\hat\tau} = -\chi a + a^3\frac{\langle\overline{U}'|\overline{U}'''\rangle}{\varepsilon_c\langle\overline{U}'|\overline{U}'\rangle} - \varepsilon_c\frac{\langle\overline{U}'|\eta\rangle}{\langle\overline{U}'|\overline{U}'\rangle}. \tag{4.7}$$

Finally, rescaling p, a, and η, we obtain the pair of equations

$$\begin{aligned} p_t &= a, \\ a_t &= (\varepsilon_c - \varepsilon)a + \frac{\langle\overline{U}'|\overline{U}'''\rangle}{\varepsilon_c\langle\overline{U}'|\overline{U}'\rangle}a^3 - \varepsilon_c\frac{\langle\overline{U}'|\eta\rangle}{\langle\overline{U}'|\overline{U}'\rangle}. \end{aligned} \tag{4.8}$$

Note that $\overline{U} = \overline{U}(x-p)$, so that the final coefficient on the right-hand side of (4.8) will be p-dependent in the case of an inhomogeneous input $\eta = \eta(x)$.

Cusp bifurcation for homogeneous inputs. It is clear from (4.8) that when $\eta = 0$ we recover the pitchfork bifurcation of a stationary front as found in section 3. In particular, for $\varepsilon < \varepsilon_c$ there are three constant speed solutions of (4.8) such that

$a_t = 0, P_t = a = c$, corresponding to an unstable stationary front and a pair of stable counterpropagating fronts with speeds

$$c = \pm\sqrt{(\varepsilon_c - \varepsilon)\varepsilon_c \frac{\langle \overline{U}' | \overline{U}' \rangle}{|\langle \overline{U}' | \overline{U}''' \rangle|}}. \tag{4.9}$$

If η is nonzero but constant, on the other hand, the final term on the right-hand side of (4.8) reduces to the constant coefficient $\varepsilon_c \eta (f(U_+) - f(U_-))/\langle \overline{U}' | \overline{U}' \rangle$, and the pitchfork bifurcation unfolds to a saddle-node bifurcation. There are two saddle-node lines in the (η, ε)-plane corresponding to the condition $dG(a)/da = 0$, where $a_t = G(a)$:

$$\eta_{sn} = \pm \frac{2}{3\sqrt{3}} \frac{(\varepsilon_c - \varepsilon)^{3/2}}{\varepsilon_c^{1/2}} \frac{\langle \overline{U}' | \overline{U}' \rangle^{3/2}}{(f(U_+) - f(U_-))|\langle \overline{U}' | \overline{U}''' \rangle|^{1/2}}, \tag{4.10}$$

and the corresponding speed along these lines is

$$c_{sn} = \pm\sqrt{(\varepsilon_c - \varepsilon)\varepsilon_c \frac{\langle \overline{U}' | \overline{U}' \rangle}{3|\langle \overline{U}' | \overline{U}''' \rangle|}}. \tag{4.11}$$

Hopf bifurcation for a weak inhomogeneity. The introduction of a weak input inhomogeneity can lead to a Hopf instability of the stationary front. We shall illustrate this by considering the particular example of the step inhomogeneity

$$\eta(x) = \begin{cases} s/2 & \text{if } x \leq 0, \\ -s/2 & \text{if } x > 0 \end{cases} \tag{4.12}$$

with $s > 0$. For such an input we find that

$$\langle \overline{U}' | \eta \rangle = \frac{s}{2}[2f(\overline{U}(-p)) - f(U_+) - f(U_-)]. \tag{4.13}$$

Recall from section 2 that when $h = 0.5$ the homogeneous network with f given by (1.2) supports a stationary front solution for which $U_\pm = \pm 0.5/(1+\beta)$, and $\overline{U}(0) = 0$ such that $f(U_+) + f(U_-) = 2f(0)$. Hence, (4.8) has a fixed point at $p = 0, a = 0$. Linearization about this fixed point shows that there is a Hopf bifurcation of the stationary front at $\varepsilon = \varepsilon_c$ with Hopf frequency

$$\omega_H = \sqrt{\frac{s\varepsilon_c f'(0)|\overline{U}'(0)|}{\langle \overline{U}' | \overline{U}' \rangle}}. \tag{4.14}$$

The supercritical or subcritical nature of the Hopf bifurcation can then be determined by evaluating higher order terms in a, p. However, this is complicated by the fact that we do not have an analytical expression for the stationary front solution $\overline{U}$, in contrast to the case of a reaction–diffusion equation with a cubic nonlinearity [2]. (Note that, as in the case of reaction–diffusion equations [2], one can develop a more intricate perturbation analysis that takes into account $\mathcal{O}(\delta^2)$ inhomogeneities and corresponding shifts in the Hopf bifurcation point. Here we have followed a simpler approach in order to illustrate the basic ideas underlying the perturbative treatment of the integro-differential equation (1.1).)

5. Exactly solvable model. We now consider the high gain limit $\gamma \to \infty$, for which (1.2) reduces to $f(u) = H(u-\kappa)$, where H is the Heaviside function $H(u) = 1$ if $u > 0$ and $H(u) = 0$ if $u \le 0$. The advantage of using a threshold nonlinearity is that explicit analytical expressions for front solutions can be obtained, which allows us to derive conditions for the Hopf instability of a stationary front without any restrictions on the size of the input inhomogeneity. Numerical simulations of the full system establish that the bifurcation is supercritical and that it generates an oscillatory modulation of the stationary front in the form of a breather [3]. (For a corresponding analysis of reaction–diffusion equations, see Prat and Li [13].)

5.1. Traveling fronts (homogeneous case). We begin by deriving exact traveling front solutions of (1.1) for $f(u) = H(u-\kappa)$ and a homogeneous input $I(x) = 0$. That is, we seek a solution of the form $u(x,t) = U(\xi)$, $\xi = x - ct$, $c > 0$, such that $U(0) = \kappa$, $U(\xi) < \kappa$ for $\xi > 0$ and $U(\xi) > \kappa$ for $\xi < 0$. Setting $v(x,t) = V(\xi)$, we then have

$$-cU'(\xi) + U(\xi) = \int_{-\infty}^{0} w(\xi - \xi')d\xi' - \beta V(\xi), \tag{5.1}$$

$$-\frac{c}{\varepsilon}V'(\xi) = -V(\xi) + U(\xi). \tag{5.2}$$

Differentiating the first equation and substituting into the second, we obtain a second-order ODE with boundary conditions at $\xi = 0$ and $\pm\infty$:

$$\begin{aligned} -c^2U''(\xi) + c[1+\varepsilon]U'(\xi) - \varepsilon[1+\beta]U(\xi) &= -cw(\xi) - \varepsilon W(\xi), \\ U(0) &= \kappa, \\ U(\mp\infty) &= U_{\pm}, \end{aligned} \tag{5.3}$$

where

$$W(\xi) = \int_{\xi}^{\infty} w(y)dy. \tag{5.4}$$

Here $U_{\pm}$ are the homogeneous fixed point solutions

$$U_+ = \frac{1}{1+\beta}, \quad U_- = 0. \tag{5.5}$$

We have used the fact that w has unit normalization, $W(-\infty) \equiv \int_{-\infty}^{\infty} w(y)dy = 1$. It follows that a necessary condition for the existence of a front solution is $\kappa < U_+$.

In order to establish the existence of a traveling front, we solve the boundary value problem in the domains $\xi \le 0$ and $\xi \ge 0$ and match the solutions at $\xi = 0$. For further mathematical convenience, we take the weight distribution to be an exponential function

$$w(x) = \frac{1}{2d}\mathrm{e}^{-|x|/d}, \tag{5.6}$$

where d determines the range of the synaptic interactions. We fix the spatial scale by setting $d = 1$; a typical value of d is 1 mm. We first consider the case of right-moving

waves ($c > 0$). On the domain $\xi \geq 0$, the particular solution is $U_>(\xi) = \kappa e^{-\xi}$, with κ related to the speed c according to the self-consistency condition

$$\kappa = \frac{c+\varepsilon}{2(c^2 + c[1+\varepsilon] + \varepsilon[1+\beta])}, \qquad c \geq 0. \tag{5.7}$$

In the domain $\xi \leq 0$ the solution consists of complementary and particular parts:

$$U_<(\xi) = \mathcal{A}_+ e^{\mu_+ \xi} + \mathcal{A}_- e^{\mu_- \xi} + \mathcal{A} e^{\xi} + U_+, \tag{5.8}$$

where

$$\mu_\pm = \frac{1}{2c}\left[1 + \varepsilon \pm \sqrt{(1+\varepsilon)^2 - 4\varepsilon(1+\beta)}\right]. \tag{5.9}$$

The coefficient $\mathcal{A}$ is obtained by direct substitution into the differential equation for U, whereas the coefficients $\mathcal{A}_\pm$ are determined by matching solutions at the boundary $\xi = 0$, that is, $U_<(0) = \kappa$ and $U_<'(0) = -\kappa$. Thus we find

$$\mathcal{A} = \frac{c-\varepsilon}{2(c^2 - c[1+\varepsilon] + \varepsilon[1+\beta])}, \tag{5.10}$$

$$\mathcal{A}_+ = \frac{\mu_- U_+ + (\mu_- - 1)\mathcal{A} - (1+\mu_-)\kappa}{\mu_+ - \mu_-}, \tag{5.11}$$

$$\mathcal{A}_- = \frac{-\mu_+ U_+ + (1-\mu_+)\mathcal{A} + (1+\mu_+)\kappa}{\mu_+ - \mu_-}. \tag{5.12}$$

In the limit $\beta \to 0$ we recover the standard result for an excitatory network without feedback [5]:

$$U(\xi) = \begin{cases} \dfrac{1}{2(c+1)} e^{-\xi} & \text{for } \xi > 0, \\ 1 + (\kappa - 1)e^{\xi/c} + \dfrac{1}{2(c-1)}\left[e^{\xi} - e^{\xi/c}\right] & \text{for } \xi < 0 \end{cases} \tag{5.13}$$

with

$$\kappa = \frac{1}{2(c+1)}, \qquad c \geq 0. \tag{5.14}$$

A similar analysis can be carried out for left-moving waves. Now the speed c is determined by the particular solution in the domain $\xi \leq 0$, which takes the form $U_<(\xi) = -\hat{\kappa} e^{\xi} + U_+$ with $\hat{\kappa} = (1+\beta)^{-1} - \kappa$. This leads to the self-consistency condition

$$\hat{\kappa} = -\frac{c-\varepsilon}{2(c^2 - c[1+\varepsilon] + \varepsilon[1+\beta])}, \qquad c \leq 0. \tag{5.15}$$

The existence of traveling front solutions can now be established by finding positive real solutions of (5.7) and negative real solutions of (5.15). For concreteness, we will assume that the threshold κ is fixed and determine the solution branches as a

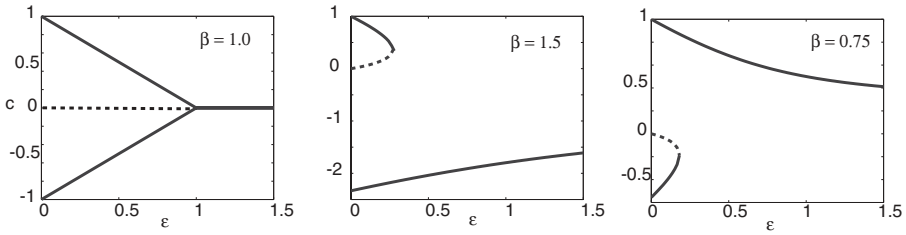

FIG. 5.1. *Plot of wavefront speed c as a function of ε for various values of β and a fixed threshold $\kappa = 0.25$: (i) $2\kappa(1+\beta) = 1$, (ii) $2\kappa(1+\beta) > 1$, (iii) $2\kappa(1+\beta) < 1$. Stable (unstable) branches are shown as solid (dashed) curves.*

function of the feedback parameters ε, β with $1/\kappa - 1 > \beta > 0$. The roots of (5.7) and (5.15) can be written explicitly as

$$c = \frac{1}{2}\left[-\left(1+\varepsilon-\frac{1}{2\kappa}\right) \pm \sqrt{\left(1+\varepsilon-\frac{1}{2\kappa}\right)^2 - 4\varepsilon\left(1+\beta-\frac{1}{2\kappa}\right)}\right] \tag{5.16}$$

and

$$c = \frac{1}{2}\left[\left(1+\varepsilon-\frac{1}{2\hat{\kappa}}\right) \pm \sqrt{\left(1+\varepsilon-\frac{1}{2\hat{\kappa}}\right)^2 - 4\varepsilon\left(1+\beta-\frac{1}{2\hat{\kappa}}\right)}\right]. \tag{5.17}$$

Using the fact that $\operatorname{sign}\left(1+\beta-\frac{1}{2\kappa}\right) = -\operatorname{sign}\left(1+\beta-\frac{1}{2\hat{\kappa}}\right)$, we find that there are three bifurcation scenarios, as shown in Figure 5.1:

(i) If $2\kappa(1+\beta) = 1$, then there exists a stationary front for all ε. At a critical value of ε the stationary front undergoes a pitchfork bifurcation, leading to the formation of a left- and a right-moving wave. This is the high gain limit of the front bifurcation analyzed in section 3 for smooth f.

(ii) If $2\kappa(1+\beta) > 1$, then there is a single left-moving wave for all ε. There also exists a pair of right-moving waves that annihilate in a saddle-node bifurcation at a critical value of ε that approaches zero as $\beta \to 0$.

(iii) If $2\kappa(1+\beta) < 1$, then there is a single right-moving wave for all ε. There also exists a pair of left-moving waves that annihilate in a saddle-node bifurcation at a critical value of ε that approaches zero as $\beta \to 0$.

5.2. Stability analysis of stationary fronts (inhomogeneous case). Stationary front solutions of (1.1) with $f(u) = H(u-\kappa)$ in the case of an inhomogeneous input $I(x)$ satisfy the equation

$$(1+\beta)U(x) = \int_{-\infty}^{x_0} w(x-x')dx' + I(x). \tag{5.18}$$

Suppose that $I(x)$ is a monotonically decreasing function of x. Since the system is no longer translation invariant, the position of the front is pinned to a particular location x_0, where $U(x_0) = \kappa$. Monotonicity of $I(x)$ ensures that $U(x) > \kappa$ for $x < x_0$ and $U(x) < \kappa$ for $x > x_0$. The center x_0 satisfies

$$(1+\beta)\kappa = \frac{1}{2} + I(x_0) \tag{5.19}$$

under the normalization $\int_0^\infty w(y)dy = 1/2$. Equation (5.19) implies that in contrast to the homogeneous case, there exists a stationary front over a range of threshold values (for fixed β); changing the threshold κ simply shifts the position of the center x_0. In the particular case of the exponential weight distribution (5.6), we have

$$(1+\beta)U(x) = \begin{cases} \dfrac{\mathrm{e}^{x_0-x}}{2} + I(x), & x > x_0, \\ 1 - \dfrac{\mathrm{e}^{x-x_0}}{2} + I(x), & x < x_0. \end{cases} \tag{5.20}$$

If the stationary front is stable, then it will prevent wave propagation. Stability is determined by writing $u(x,t) = U(x) + p(x,t)$ and $v(x,t) = V(x) + q(x,t)$ with $V(x) = U(x)$ and expanding (1.1) to first-order in $(p,\ q)$:

$$\frac{\partial p(x,t)}{\partial t} = -p(x,t) + \int_{-\infty}^{\infty} w(x-x')H'(U(x'))p(x',t)dx' - \beta q(x,t),$$

$$\frac{1}{\varepsilon}\frac{\partial q(x,t)}{\partial t} = -q(x,t) + p(x,t). \tag{5.21}$$

We assume that $p, q \in L^2(\mathbf{R})$. The spectrum of the associated linear operator is found by taking $p(x,t) = \mathrm{e}^{\lambda t}p(x)$ and $q(x,t) = \mathrm{e}^{\lambda t}q(x)$. Using the identity

$$\frac{dH(U(x))}{dU} = \frac{\delta(x-x_0)}{|U'(x_0)|} \tag{5.22}$$

we obtain the equation

$$(\lambda+1)p(x) = \frac{w(x-x_0)}{|U'(x_0)|}p(x_0) - \frac{\varepsilon\beta p(x)}{\lambda+\varepsilon}. \tag{5.23}$$

Equation (5.23) has two classes of solution. The first consists of any function $p(x)$ such that $p(x_0) = 0$, for which $\lambda = \lambda_\pm^{(0)}$, where

$$\lambda_\pm^{(0)} = \frac{-(1+\varepsilon) \pm \sqrt{(1+\varepsilon)^2 - 4\varepsilon(1+\beta)}}{2}. \tag{5.24}$$

Note that $\lambda_\pm^{(0)}$ belong to the essential spectrum since they have infinite multiplicity. The second class of solution is of the form $p(x) = Aw(x-x_0)$, $A \neq 0$, for which λ is given by the roots of the equation

$$\lambda + 1 + \frac{\varepsilon\beta}{\lambda+\varepsilon} = \frac{1}{2|U'(x_0)|}. \tag{5.25}$$

Since

$$U'(x_0) = \frac{1}{1+\beta}\left[I'(x_0) - \frac{1}{2}\right], \tag{5.26}$$

it follows that $\lambda = \lambda_\pm$, where

$$\lambda_\pm = \frac{-\Lambda \pm \sqrt{\Lambda^2 - 4(1-\Gamma)\varepsilon(1+\beta)}}{2} \tag{5.27}$$

with

$$\Lambda = 1 + \varepsilon - (1+\beta)\Gamma \tag{5.28}$$

and

$$\Gamma = \frac{1}{1+2D}, \quad D = |I'(x_0)|. \tag{5.29}$$

We have used the fact that $I'(x_0) \leq 0$. The eigenvalues $\lambda_\pm$ determine the discrete spectrum.

5.3. Hopf bifurcation to a breathing front. Equation (5.27) implies that the stationary front is locally stable, provided that $\Lambda > 0$ or, equivalently, the gradient of the inhomogeneous input at x_0 satisfies

$$D > D_c \equiv \frac{1}{2}\frac{\beta - \varepsilon}{1+\varepsilon}. \tag{5.30}$$

Since $D \geq 0$, it follows that the front is stable when $\beta < \varepsilon$, that is, when the feedback is sufficiently weak or fast. On the other hand, if $\beta > \varepsilon$, then there is a Hopf bifurcation at the critical gradient $D = D_c$. The corresponding critical Hopf frequency is

$$\omega_H = \sqrt{\frac{2D_c\varepsilon(1+\beta)}{2D_c+1}} = \sqrt{\varepsilon(\beta-\varepsilon)}. \tag{5.31}$$

Note that the frequency depends only on the size and rate of the negative feedback but is independent of the details of the synaptic weight distribution and the size of the input. This should be contrasted with the corresponding Hopf frequency in the case of a smooth nonlinearity f and a weak step-inhomogeneity; see (4.14). The latter depends on the input amplitude and the form of the stationary solution $\overline{U}$, which itself depends on the weight distribution w.

In order to investigate the nature of solutions around the Hopf bifurcation point, we consider the particular example of a smooth ramp inhomogeneity

$$I(x) = -\frac{s}{2}\tanh(\gamma x), \tag{5.32}$$

where s is the size of the step and γ determines its steepness. A stationary front will exist provided that

$$s > \bar{s} \equiv |1 - 2\kappa(1+\beta)|. \tag{5.33}$$

The gradient $D = s\gamma\,\mathrm{sech}^2(\gamma x_0)/2$ depends on x_0, which is itself dependent on β and κ through (5.19). Using the identity $\mathrm{sech}^2 x = 1 - \tanh^2 x$, it follows that

$$D = \frac{\gamma}{2s}\left(s^2 - \bar{s}^2\right). \tag{5.34}$$

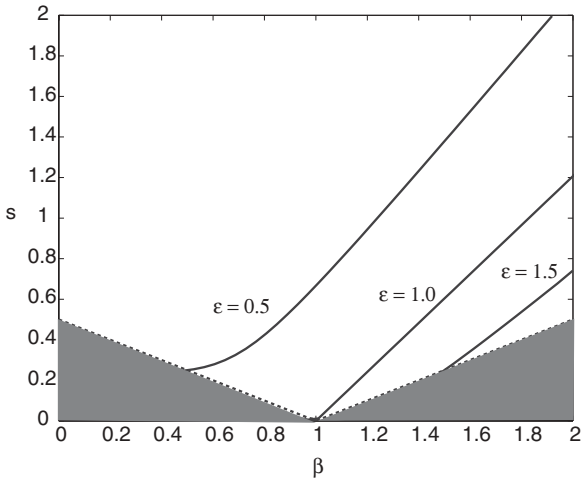

FIG. 5.2. *Stability phase diagram for a stationary front in the case of a step input* $I(x) = -s\tanh(\gamma x)/2$, *where* γ *is the steepness of the step and* s *its height. Hopf bifurcation lines (solid curves) in* $s-\beta$ *parameter space are shown for various values of* ε. *In each case the stationary front is stable above the line and unstable below it. The shaded area denotes the region of parameter space where a stationary front solution does not exist. The threshold* $\kappa = 0.25$ *and* $\gamma = 0.5$.

Combining (5.30) and (5.34), we obtain an expression for the critical value of s that determines the Hopf bifurcation points:

$$s_c = \frac{1}{2\gamma}\left[\frac{\beta-\varepsilon}{1+\varepsilon} + \sqrt{\left(\frac{\beta-\varepsilon}{1+\varepsilon}\right)^2 + 4\bar{s}^2\gamma^2}\right]. \tag{5.35}$$

The critical height s_c is plotted as a function of β for various values of ε and fixed κ, γ in Figure 5.2. Note that in the homogeneous case ($s = 0$) a stationary solution exists only at the particular value of β given by $\beta = 1/(2\kappa) - 1$. This solution is stable for $\varepsilon > \beta$ and unstable for $\varepsilon < \beta$, which is consistent with the pitchfork bifurcation shown in Figure 5.1. Close to the front bifurcation $\varepsilon = \beta$, the Hopf bifurcation occurs in the presence of a weak input inhomogeneity, which is the case considered in section 2. Now, however, it is possible to determine the bifurcation curve without any restrictions on the size of the input.

Numerically solving the full system of equations (1.1) for a step input $I(x)$, exponential weights $w(x)$, and threshold nonlinearity $f(u) = H(u-\kappa)$ shows that the Hopf bifurcation is supercritical, in which there is a transition to a small amplitude breather whose frequency of oscillation is approximately equal to the Hopf frequency ω_H. As the input amplitude s is reduced beyond the Hopf bifurcation point, the amplitude of the oscillation increases until the breather itself becomes unstable and there is a secondary bifurcation to a traveling front. This is illustrated in Figure 5.3, which shows a space-time plot of the developing breather as the input amplitude is slowly reduced. Note that analogous results have been obtained for pulses in the presence of stationary Gaussian inputs, where a reduction in the input amplitude induces a Hopf bifurcation to a pulse-like breather [3, 6]. Interestingly, the localized breather can itself undergo a secondary instability leading to the periodic emission of traveling waves. In one dimension such waves consist of pairs of counterpropagating pulses, whereas in two dimensions the waves are circular target patterns [6].

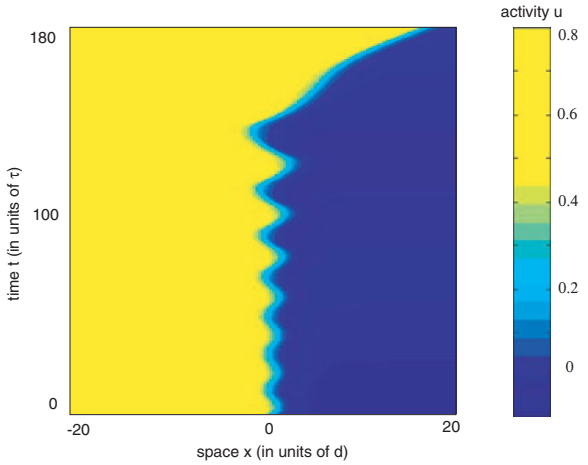

FIG. 5.3. *Breather-like solution arising from a Hopf instability of a stationary front due to a slow reduction in the size s of the step input inhomogeneity* (5.32). *Here* $\varepsilon = 0.5, \gamma = 0.5, \beta = 1, \kappa = 0.25$. *The input amplitude* $s = 2$ *at* $t = 0$ *and* $s = 0$ *at* $t = 180$. *The amplitude of the oscillation steadily grows until it destabilizes at* $s \approx 0.05$, *leading to the generation of a traveling front.*

5.4. Locking to a moving input. We conclude our analysis of the exactly solvable model by considering the effects of a moving input stimulus. This is interesting from a number of viewpoints. First, introducing a persistent stationary input into an in vitro cortical slice can damage the tissue, whereas a moving input (at least if it is localized) will not. Second, in vivo inputs into the intact cortex are typically nonstationary, as exemplified by inputs to the visual cortex induced by moving visual stimuli. We consider the particular problem of whether or not a traveling front can lock to a step-like input $I(x) = I_0\chi(x - vt)$ traveling with constant speed v, where

$$\chi(x) = \begin{cases} -1, & x > 0, \\ 0, & x = 0, \\ +1, & x < 0. \end{cases}$$

Such a front moves at the same speed as the input but may be shifted in space relative to the input.

We proceed by introducing the traveling wave coordinate $\xi = x - vt$ and deriving existence conditions for a front solution $U(\xi)$ satisfying $U(\xi) \to 0$ as $\xi \to \infty$, $U(\xi) \to (1+\beta)^{-1}$ as $\xi \to -\infty$, and $U(\xi_0) = \kappa$. Substituting into (1.1) gives

$$-vU'(\xi) = -U(\xi) + \int_{-\infty}^{\xi_0} w(\xi - \eta)d\eta - \beta V(\xi) + I_0\chi(\xi), \tag{5.36}$$

$$-vV'(\xi) = \epsilon(-V(\xi) + U(\xi)). \tag{5.37}$$

Setting $W(\xi) = \int_{\xi}^{\infty} w(\eta)d\eta$, we can rewrite this pair of equations in the matrix form

$$\mathbf{LS} \equiv \begin{pmatrix} vU' - U - \beta V \\ vV' + \epsilon U - \epsilon V \end{pmatrix} = -\begin{pmatrix} N_{\mathrm{E}} \\ 0 \end{pmatrix}, \tag{5.38}$$

where

$$\mathbf{S} = (U, V)^T, \qquad N_{\mathrm{E}}(\xi) = W(\xi - \xi_0) + I_0\chi(\xi). \tag{5.39}$$

We use variation of parameters to solve this linear equation. The homogeneous problem $\mathbf{L}S = 0$ has the two linearly independent solutions,

$$\mathbf{S}_+(\xi) = \begin{pmatrix} \beta \\ m_+ - 1 \end{pmatrix} \exp(\mu_+ \xi), \tag{5.40}$$

$$\mathbf{S}_-(\xi) = \begin{pmatrix} \beta \\ m_- - 1 \end{pmatrix} \exp(\mu_- \xi), \tag{5.41}$$

where

$$\mu_\pm = \frac{m_\pm}{v}, \qquad m_\pm = \frac{1}{2}\Big(1 + \epsilon \pm \sqrt{(1-\epsilon)^2 - 4\epsilon\beta}\Big).$$

By variation of parameters we define

$$\mathbf{S}(\xi) = [\mathbf{S}_+(\xi)|\mathbf{S}_-(\xi)] \begin{pmatrix} a(\xi) \\ b(\xi) \end{pmatrix},$$

where $[\mathbf{A}|\mathbf{B}]$ denotes the matrix whose first column is defined by the vector $\mathbf{A}$ and whose second column is defined by the vector $\mathbf{B}$. Then

$$\begin{aligned} \mathbf{LS} &= v\frac{\partial}{\partial \xi}\left([\mathbf{S}_+(\xi)|\mathbf{S}_-(\xi)] \begin{pmatrix} a(\xi) \\ b(\xi) \end{pmatrix}\right) - \begin{pmatrix} 1 & \beta \\ -\epsilon & \epsilon \end{pmatrix}\left([\mathbf{S}_+(\xi)|\mathbf{S}_-(\xi)] \begin{pmatrix} a(\xi) \\ b(\xi) \end{pmatrix}\right) \\ &= v[\mathbf{S}_+(\xi)|\mathbf{S}_-(\xi)]\frac{\partial}{\partial \xi} \begin{pmatrix} a(\xi) \\ b(\xi) \end{pmatrix}, \end{aligned} \tag{5.42}$$

since $\mathbf{LS}_\pm = 0$. Thus (5.38) reduces to

$$[\mathbf{S}_+(\xi)|\mathbf{S}_-(\xi)]\frac{\partial}{\partial \xi} \begin{pmatrix} a(\xi) \\ b(\xi) \end{pmatrix} = -\frac{1}{v} \begin{pmatrix} N_{\rm E} \\ 0 \end{pmatrix}. \tag{5.43}$$

The matrix $[\mathbf{S}_+(\xi)|\mathbf{S}_-(\xi)]$ is invertible. Introducing the vector-valued functions

$$\mathbf{Z}_+(\xi) = \begin{pmatrix} 1 - m_- \\ \beta \end{pmatrix} \exp(-\mu_+ \xi), \tag{5.44}$$

$$\mathbf{Z}_-(\xi) = -\begin{pmatrix} 1 - m_+ \\ \beta \end{pmatrix} \exp(-\mu_- \xi), \tag{5.45}$$

we have

$$[\mathbf{S}_+|\mathbf{S}_-][\mathbf{Z}_+|\mathbf{Z}_-]^{\rm T} = [\mathbf{Z}_+|\mathbf{Z}_-]^{\rm T}[\mathbf{S}_+|\mathbf{S}_-] = \beta(m_+ - m_-)\mathrm{I},$$

where I denotes the identity matrix. Multiplying (5.43) by $[\mathbf{Z}_+|\mathbf{Z}_-]^{\rm T}$ finally yields the first-order equation

$$\frac{\partial}{\partial \xi} \begin{pmatrix} a(\xi) \\ b(\xi) \end{pmatrix} = -\frac{1}{v\beta(m_+ - m_-)}[\mathbf{Z}_+(\xi)|\mathbf{Z}_-(\xi)]^{\rm T} \begin{pmatrix} N_{\rm E}(\xi) \\ 0 \end{pmatrix}. \tag{5.46}$$

In order to solve (5.46) we need to specify the sign of v. First, suppose that $v > 0$, which corresponds to a right-moving front. Integrating over the interval $[\xi, \infty)$ gives

$$\begin{pmatrix} a(\xi) \\ b(\xi) \end{pmatrix} = \begin{pmatrix} a_\infty \\ b_\infty \end{pmatrix} + \frac{1}{v\beta(m_+ - m_-)} \int_\xi^\infty [\mathbf{Z}_+(\eta)|\mathbf{Z}_-(\eta)]^{\rm T} \begin{pmatrix} N_{\rm E}(\eta) \\ 0 \end{pmatrix} d\eta,$$

where a_∞, b_∞ denote the values of a, b at ∞. Since we seek a bounded solution $\mathbf{S}(\xi)$, we must require that $a_\infty = b_\infty = 0$. Hence the solution is

$$\begin{pmatrix} a(\xi) \\ b(\xi) \end{pmatrix} = \frac{1}{v\beta(m_+ - m_-)} \int_\xi^\infty [\mathbf{Z}_+(\eta)|\mathbf{Z}_-(\eta)]^{\mathrm{T}} \begin{pmatrix} N_{\mathrm{E}}(\eta) \\ 0 \end{pmatrix} d\eta,$$

so that

$$\mathbf{S}(\xi) = \frac{1}{v\beta(m_+ - m_-)} [\mathbf{S}_+(\xi)|\mathbf{S}_-(\xi)] \int_\xi^\infty [\mathbf{Z}_+(\eta)|\mathbf{Z}_-(\eta)]^{\mathrm{T}} \begin{pmatrix} N_{\mathrm{E}}(\eta) \\ 0 \end{pmatrix} d\eta. \tag{5.47}$$

Further simplification occurs by introducing the functions

$$M_\pm(\xi) = \frac{1}{v} \left(\frac{1}{m_+ - m_-} \right) \int_\xi^\infty e^{\mu_\pm(\xi - \eta)} N_{\mathrm{E}}(\eta) d\eta.$$

We can then express the solution for $(U(\xi), V(\xi))$ as follows:

$$U(\xi) = (1 - m_-)M_+(\xi) - (1 - m_+)M_-(\xi), \tag{5.48}$$

$$V(\xi) = \beta^{-1}(m_+ - 1)(1 - m_-) \left[M_+(\xi) - M_-(\xi) \right]. \tag{5.49}$$

To ensure that such a front exists we require that $U(\xi_0) = \kappa$, i.e.,

$$\kappa = (1 - m_-)M_+(\xi_0) - (1 - m_+)M_-(\xi_0). \tag{5.50}$$

Taking $w(x) = \mathrm{e}^{-|x|}/2$ so that

$$W(\xi) = \begin{cases} 1 - \dfrac{1}{2} e^{\xi}, & \xi < 0, \\ \\ \dfrac{1}{2} e^{-\xi}, & \xi \geq 0, \end{cases}$$

we can calculate $M_\pm(\xi_0)$ explicitly as

$$M_\pm(\xi_0) = \frac{1}{(m_+ - m_-)} \left(\frac{1}{2(v + m_\pm)} - \frac{1}{m_\pm} F(\xi_0) \right),$$

where

$$F(\xi_0) = \begin{cases} I_0(2e^{\mu_\pm \xi_0} - 1), & \xi_0 < 0, \\ \\ I_0, & \xi_0 \geq 0. \end{cases}$$

The case of a left-moving front for which $v < 0$ follows along similar lines by integrating (5.46) over $(-\infty, \xi_0]$:

$$U(\xi) = (m_- - 1)\breve{M}_+(\xi) - (m_+ - 1)\breve{M}_-(\xi), \tag{5.51}$$

$$V(\xi) = \beta^{-1}(m_+ - 1)(1 - m_-) \left[\breve{M}_+(\xi) - \breve{M}_-(\xi) \right], \tag{5.52}$$

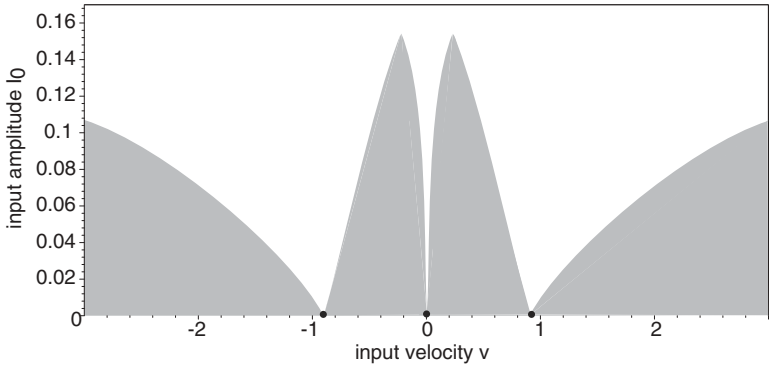

FIG. 5.4. *Locking of a traveling front to a moving step input with velocity v and amplitude I_0. Other parameter values are $\beta = 1, \varepsilon = 0.1, \kappa = 0.25$. Unshaded regions show where locking can occur in the (v, I_0)-plane. When $I_0 = 0$ there are three front solutions corresponding to a stationary front ($v = 0$) and two counterpropagating fronts, which is consistent with the front bifurcation shown in Figure* 5.1. *Each of these solutions forms the vertex of a distinct locking region whose width increases monotonically with I_0 so that ultimately the locking regions merge.*

where

$$\breve{M}_{\pm}(\xi_0) = \frac{1}{(m_+ - m_-)} \left(\frac{1}{2} \frac{m_{\pm} - 2v}{m_{\pm}(v - m_{\pm})} - \frac{1}{m_{\pm}} G(\xi_0) \right)$$

and

$$G(\xi_0) = \begin{cases} -I_0, & \xi_0 < 0, \\ I_0(1 - 2e^{\mu_{\pm}\xi_0}), & \xi_0 \geq 0. \end{cases}$$

This leads to the following threshold condition for $v < 0$:

$$\kappa = (m_- - 1)\breve{M}_+(\xi_0) - (m_+ - 1)\breve{M}_-(\xi_0). \tag{5.53}$$

We can now numerically solve (5.50) and (5.53) to determine the range of input velocities v and input amplitudes I_0 for which locking occurs. For the sake of illustration, we assume the threshold condition $2\kappa(1 + \beta) = 1$ and take $\varepsilon < \beta$. This ensures that, in the absence of any input, there exists an unstable stationary front and a pair of stable counterpropagating waves (see Figure 5.1). The continuation of these stationary and traveling fronts as I_0 increases from zero is shown in Figure 5.4. Since $2\kappa(1+\beta) = 1$, equations (5.50) and (5.53) are equivalent under the interchange $v \to -v$ and $\xi_0 \to -\xi_0$. This implies that the locking regions are symmetric with respect to v. For nonzero v the traveling front is shifted relative to the input such that $\xi_0 < 0$ when $v > 0$ and $\xi_0 > 0$ when $v < 0$. In other words, the wave is dragged by the input.

Figure 5.4 determines where locking can occur but not whether the resulting traveling wave is stable or unstable. Indeed, the stability analysis of traveling fronts is considerably more involved than that of stationary fronts. Nevertheless, we expect that for sufficiently small I_0 the locking regions around the counterpropagating fronts are stable, whereas the central region containing the stationary front is unstable. On the other hand, since $\beta > \varepsilon$, we know that the stationary front is stable for large inputs I_0 and undergoes a Hopf bifurcation as I_0 is reduced. This suggests that the Hopf bifurcation point at $v = 0$ lies on a Hopf curve within the locking region so that

a traveling front locked to a moving input can also be destabilized as the strength of the input is reduced (or as the input velocity changes relative to the intrinsic velocity of waves in the homogeneous network). Recently, Zhang [19] analyzed the asymptotic stability of traveling wave solutions of (1.1) in the case of homogeneous inputs by deriving the associated Evans function and evaluating it in the singular limit $\varepsilon \ll 1$. In future work we will extend this analysis to the case of inhomogeneous inputs and finite ε, thus determining the stability of the locking regions shown in Figure 5.4. We will also construct corresponding locking regions for traveling pulses in the presence of moving Gaussian inputs, and numerically explore the types of oscillatory solutions bifurcating from these waves.

Acknowledgment. We would like to thank Yue-Xian Li (University of British Columbia) for many helpful discussions regarding his work on wavefront instabilities in reaction–diffusion equations.

REFERENCES

[1] S. Amari, *Dynamics of pattern formation in lateral inhibition type neural fields*, Biol. Cybern., 27 (1977), pp. 77–87.

[2] M. Bode, *Front-bifurcations in reaction-diffusion systems with inhomogeneous parameter distributions*, Phys. D, 106 (1997), pp. 270–286.

[3] P. C. Bressloff, S. E. Folias, A. Prat, and Y.-X. Li, *Oscillatory waves in inhomogeneous neural media*, Phys. Rev. Lett., 91 (2003), article 178101.

[4] R. D. Chervin, P. A. Pierce, and B. W. Connors, *Periodicity and directionality in the propagation of epileptiform discharges across neocortex*, J. Neurophysiol., 60 (1988), pp. 1695–1713.

[5] G. B. Ermentrout and J. B. McLeod, *Existence and uniqueness of travelling waves for a neural network*, Proc. Roy. Soc. Edinburgh Sect. A, 123 (1993), pp. 461–478.

[6] S. E. Folias and P. C. Bressloff, *Breathing pulses in an excitatory neural network*, SIAM J. Appl. Dynam. Systems, to appear.

[7] D. Golomb and Y. Amitai, *Propagating neuronal discharges in neocortical slices: Computational and experimental study*, J. Neurophysiol., 78 (1997), pp. 1199–1211.

[8] A. Hagberg and E. Meron, *Pattern formation in non-gradient reaction-diffusion systems: The effects of front bifurcations*, Nonlinearity, 7 (1994), pp. 805–835.

[9] A. Hagberg, E. Meron, I. Rubinstein, and B. Zaltzman, *Controlling domain patterns far from equilibrium*, Phys. Rev. Lett., 76 (1996), pp. 427–430.

[10] M. A. P. Idiart and L. F. Abbott, *Propagation of excitation in neural network models*, Network, 4 (1993), pp. 285–294.

[11] Y.-X. Li, *Tango waves in a bidomain model of fertilization calcium waves*, Phys. D, 186 (2003), pp. 27–49.

[12] D. J. Pinto and G. B. Ermentrout, *Spatially structured activity in synaptically coupled neuronal networks*: I. *Traveling fronts and pulses*, SIAM J. Appl. Math., 62 (2001), pp. 206–225.

[13] A. Prat and Y.-X. Li, *Stability of front solutions in inhomogeneous media*, Phys. D, 186 (2003), pp. 50–68.

[14] J. Rinzel and D. Terman, *Propagation phenomena in a bistable reaction-diffusion system*, SIAM J. Appl. Math., 42 (1982), pp. 1111–1137.

[15] J. E. Rubin, *Stability, bifurcations and edge oscillations in standing pulse solutions to an inhomogeneous reaction-diffusion system*, Proc. Roy. Soc. Edinburgh Sect. A, 129 (1999), pp. 1033–1079.

[16] P. Schutz, M. Bode, and H.-G. Purwins, *Bifurcations of front dynamics in a reaction-diffusion system with spatial inhomogeneities*, Phys. D, 82 (1995), pp. 382–397.

[17] H. R. Wilson and J. D. Cowan, *A mathematical theory of the functional dynamics of cortical and thalamic nervous tissue*, Kybernetik, 13 (1973), pp. 55–80.

[18] J.-Y. Wu, L. Guan, and Y. Tsau, *Propagating activation during oscillations and evoked responses in neocortical slices*, J. Neurosci., 19 (1999), pp. 5005–5015.

[19] L. Zhang, *On stability of traveling wave solutions in synaptically coupled neuronal networks*, Differential Integral Equations, 16 (2003), pp. 513–536.